Journal of Alloys and Compounds 509 (2011) 5720–5724

Contents lists available at ScienceDirect

Journal of Alloys and Compounds

journal homepage: www.elsevier.com/locate/jallcom

Studies on the magnetic, magnetostrictive and electrical properties of sol–gel synthesized Zn doped nickel ferrite

M. Atif[a,*], M. Nadeem[b], R. Grössinger[a], R. Sato Turtelli[a]

[a] Institut für Festkörperphysik, Technische Universität Wien, Wiedner Hauptstrasse 8-10, A-1040 Vienna, Austria
[b] EMMG, Physics Division, PINSTECH, P.O. Nilore, Islamabad, Pakistan

ARTICLE INFO

Article history:
Received 28 December 2010
Received in revised form 24 February 2011
Accepted 27 February 2011
Available online 5 March 2011

Keywords:
Ferrites
Sol–gel processes
Magnetic materials
Magnetostriction
Dielectric constant
Electrical conductivity

ABSTRACT

Zinc doped nickel ferrite i.e., $Ni_{1-x}Zn_xFe_2O_4$ ($0 \le x \le 0.6$) have been prepared by using sol–gel method. X-ray diffraction of these samples shows the presence of single-phase cubic spinel structure. The room temperature magnetic measurements showed that saturation magnetization (M_s) increases with the substitution of Zn^{2+} ions up to $x = 0.4$ and thereafter it begins to decrease, whereas magnetostriction (λ) value decreases with the addition of Zn^{2+} in the Ni–Zn ferrite. Dielectric permittivity (ε'), dielectric loss tangent ($\tan\delta$) and AC conductivity (σ_{AC}) for all the prepared samples have been studied as a function of frequency and composition in the range from 0.05 Hz to 10 MHz at room temperature. It has been observed that initially ε', $\tan\delta$ and σ_{AC} decreases with the substitution of Zn^{2+} up to $x = 0.4$ and then increases with the further addition of Zn^{2+} ions. Variation in the slope parameter s with zinc contents indicates the presence of different type of conduction mechanism in different compositions. The dielectric loss curves exhibit relaxation peaks which shift with the addition of Zn contents. The results have been explained on the basis of space charge polarization according to Maxwell–Wagner's two-layer model and the hopping of charges between Fe^{2+} and Fe^{3+} as well as between Ni^{3+} and Ni^{2+} ions at the octahedral sites.

1. Introduction

Spinel ferrites have attracted intense interest in fundamental science, especially for addressing the basic relationship between magnetic properties and their crystal chemistry and structure. They have been extensively investigated in recent years for their useful electrical and magnetic properties and applications in information storage systems, magnetic bulk cores, magnetic fluids, microwave absorbers and high frequency devices [1,2]. Among the spinel ferrites, Ni–Zn ferrite is a magnetic material that is much used by the modern electronics industry due to their high electrical resistivity, high values of magnetic permeability, low dielectric loss, together with high mechanical strength, good chemical stability, and low coercivities [3].

It is well known that nickel ferrite has an inverse spinel structure with Ni^{2+} ions at octahedral [B] sites and Fe^{3+} ions equally distributed at tetrahedral (A) and octahedral [B] sites. Whereas, zinc ferrite has a normal spinel structure with Zn^{2+} ions at A-sites and Fe^{3+} ions at B-sites. Therefore, when Ni^{2+} is substituted with Zn^{2+} in $Ni_{1-x}Zn_xFe_2O_4$, the cation distribution can be represented as $(Zn_x^{2+}Fe_{1-x}^{3+})[Ni_{1-x}^{2+}Fe_{1+x}^{3+}]O_4^{2-}$ [4]. This system has been extensively studied for various properties as well as for structural issues. It has been reported that in Ni–Zn ferrite magnetization increases with increasing zinc concentration up to $x = 0.4$ and then decreases with the further addition of zinc whereas the AC conductivity increases with zinc contents in Ni–Zn ferrite [5]. El-Sayed [6] investigated that initially electrical conductivity of Ni–Zn ferrite decreases as zinc content is increased from $x = 0.1$–0.3, whereas by further addition of zinc the conductivity increases. Abdeen [7] found that the real dielectric constant and dielectric loss increases as the zinc substitution increases in Ni–Zn ferrite, whereas Mohan et al. [8] predicted that the dielectric constants and dielectric loss decreases with increasing zinc content up to $x = 0.4$, after that there is a progressive increase with increase of zinc. These anomalies in the dielectric studies of Ni–Zn ferrite depend on the sample preparation technique, sintering temperature and holding time, chemical composition and microstructure [9,10].

A lot of work has been reported on the structural, magnetic and electrical properties of Ni–Zn ferrite [11–14]. But very few reports have been found in the literature on the magnetostrictive properties of Ni–Zn ferrite [15]. Nowadays a highly magnetostrictive and resistive ferrite phase has become an essential part of ferrite–ferroelectric magnetoelectric (ME) composites [16,17]. In order to obtain a high magnetoelectric response in ME composites, the ferrite phase should be highly magnetostrictive possessing high resistivity [18]. Therefore, focusing on these objectives we have

* Corresponding author. Tel.: +43 1 58801 13153; fax: +43 1 58801 13199.
E-mail address: matif_80@yahoo.com (M. Atif).

0925-8388/$ – see front matter © 2011 Elsevier B.V. All rights reserved.
doi:10.1016/j.jallcom.2011.02.163

prepared $Ni_{1-x}Zn_xFe_2O_4$ ($0 \le x \le 0.6$) by using the sol–gel method and reporting their structural, magnetic, magnetostrictive and electrical properties. However to the best of our knowledge, no reports have been found in the literature on the magnetostrictive properties along with the magnetic and electrical properties of the sol–gel prepared Ni–Zn ferrite. We herein report that for $x = 0.4$ composition, magnetization and strain derivative (slope of magnetostriction) shows high values whereas dielectric constant and electrical conductivity shows low trend in the $Ni_{1-x}Zn_xFe_2O_4$.

In this work, impedance spectroscopy has been employed in order to understand the effect of the zinc substitution on the dielectric permittivity, dielectric loss and electrical conductivity of the nickel ferrite. Data was collected in a wide range of frequency from 0.05 Hz to 10 MHz at room temperature. Complex dielectric permittivity ε^* and loss tangent $\tan\delta$ were calculated as: $\varepsilon^* = \varepsilon^{|} - j\varepsilon^{\|}$ and $\tan\delta = \varepsilon^{\|}/\varepsilon^{|}$. Complex ac conductivity was derived as $\sigma^*_{ac} = \sigma^{|}_{ac} + j\sigma^{\|}_{ac} = 1/\omega\varepsilon_0\varepsilon^* \tan\delta$ where $\omega = 2\pi f$ is the angular frequency, ε_0 is the free permittivity and superscripts | and ‖ are used for real and imaginary part of the complex electrical quantities.

2. Experimental

$Ni_{1-x}Zn_xFe_2O_4$ ($x = 0$, 0.25, 0.4, 0.5 and 0.6) were synthesized by a sol–gel method. The chemical reagents used in the preparation were $Fe(NO_3)_3{\cdot}9H_2O$, $Zn(NO_3)_2{\cdot}6H_2O$, $Ni(NO_3)_2{\cdot}6H_2O$, citric acid and distilled water. The nitrates were used in stoichiometric amounts and the total metal concentration was 1 mol/l. The molar ratio between total metal ions and citric acid was 1. First, the starting mixture containing nitrates and citric acid were dissolved in 150 ml distilled water. The solutions were heated to a temperature of 80 °C on a hot plate with vigorous stirring until the gel was formed. Afterwards, the hot plate was heated up to 200 °C and allowed the gel to burn in a self-propagating combustion manner until the gel was burnt out completely to form a loose powder. The loose powder was pre-sintered at 500 °C for 3 h then pressed under a pressure of 5 tons/cm^2. Finally, the pressed pellets were sintered at 1200 °C for 12 h followed by furnace cooling.

Structural characterization was performed by X-ray diffractometer (XRD) having CuKα radiation (1.5418 Å). The intensities were recorded from $10^\circ < 2\theta < 100^\circ$ with a scan step size of 0.02°. The field dependence of magnetization was measured by using a Physical Property Measurement System (PPMS-9T, Quantum Design) applying a magnetic field of 5 T. Linear magnetostriction measurements at room temperature were performed by a strain gauge method using an ac-bridge (50 kHz bridge; HBM Type KWS 85A1) in a pulsed field magnetometer, which exhibits a maximum magnetic field, $\mu_0 H_{max}$, of 5 T and pulse duration of 50 ms. Impedance spectroscopy on sintered pellet of $Ni_{1-x}Zn_xFe_2O_4$ was performed in the frequency range of 0.05 Hz–10 MHz at room temperature, using Alpha-N analyzer (Novocontrol, Germany). The surfaces on both sides of the pellet were cleaned properly and contacts were made by silver paint on opposite sides of the pellet, which were cured at 150 °C for 3 h. In order to check any possible surface effect of Ag-paste we also check with conducting emulsion and found the same result. Ag-paste requires some thermal/optical thrust to go inside the sample [19]. The leads were carefully checked for the dispersive behavior in the considered frequency range. It ensured the absence of any irrelevant inductive or capacitive coupling in the experimental frequency range. WINDETA software was used for data acquisition, which was fully automated by interfacing the analyzer with a computer.

3. Results and discussion

Fig. 1 illustrates the XRD pattern of the prepared $Ni_{1-x}Zn_xFe_2O_4$ ($0 \le x \le 0.6$) samples. All the peaks in Fig. 1 can be indexed well with the standard pattern for $NiFe_2O_4$ and $ZnFe_2O_4$ reported in PCPDF cards (# 74-2081 for $NiFe_2O_4$ and # 73-1963 for $ZnFe_2O_4$), and no un-indexed peak was observed. The lattice constant was found to increase with increasing zinc contents from 8.3416 Å to 8.4035 Å

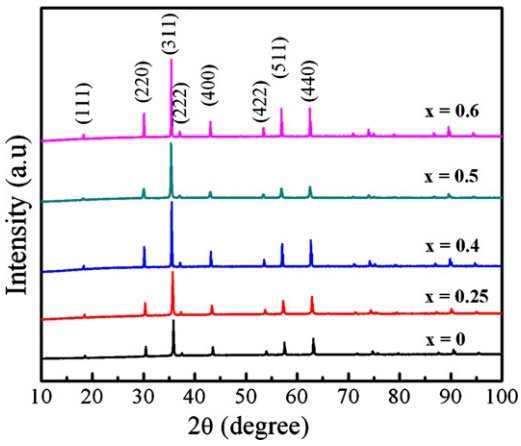

Fig. 1. X-ray diffraction patterns of $Ni_{1-x}Zn_xFe_2O_4$ ($0 \le x \le 0.6$) samples.

as 'x' varies from 0 to 0.6 in $Ni_{1-x}Zn_xFe_2O_4$. The increasing trend of lattice constant is attributed to the bigger ionic radius of Zn^{2+} ions in comparison to that of Ni^{2+} ions. Since, both Zn^{2+} ionic radius (0.82 Å) and Ni^{2+} ionic radius (0.78 Å) are larger than the interstices of A-site (0.58 Å) and B-site (0.73 Å) in spinel cubic structure. This leads to an expansion of lattice with doping Zn^{2+} ions or Ni^{2+} ions into the interstices [20]. However, the lattice expansion is more if Ni^{2+} ions are replaced by Zn^{2+} with a bigger radius than Ni^{2+} ions. Therefore, the replacement of nickel by zinc ions leads to an increase of the lattice parameter with 'x' as shown in Table 1.

The field dependent magnetization of $Ni_{1-x}Zn_xFe_2O_4$ samples with $x = 0$, 0.25, 0.4, 0.5 and 0.6 measured at 300 K in an applied field of 5 T are presented in Fig. 2. From such measurements, it has been observed that the magnetization initially increases by varying the zinc contents up to $x = 0.4$ and afterwards it begins to

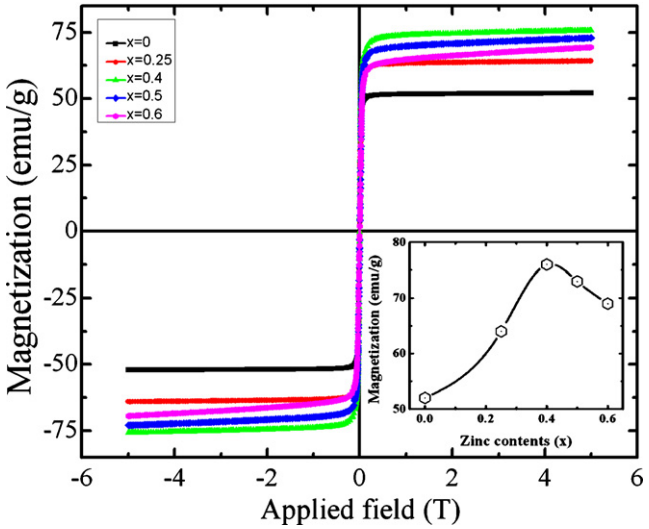

Fig. 2. Magnetization versus field behavior of $Ni_{1-x}Zn_xFe_2O_4$ at 300 K.

Table 1
Composition dependence of lattice constant (a), magnetization (M_s), linear magnetostriction (λ), slope derivative ($d\lambda/dH$), dielectric permittivity (ε'), ac conductivity (σ_{AC}), dielectric loss ($\tan\delta$) and frequency dependent parameter (s) for $Ni_{1-x}Zn_xFe_2O_4$ samples at room temperature.

Composition (x)	a (Å)	M_s (emu/g)	λ (ppm)	$d\lambda/dH$ (ppm/T)	ε' at 10 kHz	σ_{AC} ($\times 10^{-8}$ S/cm) at 10 kHz	$\tan\delta$ at 10 kHz	s
0	8.3416	52	−28	−251	12.2	11.6	2.14	0.29
0.25	8.3702	64	−20	−190	3.08	1.68	0.95	0.43
0.4	8.3776	76	−11	−212	2.77	0.84	0.45	0.57
0.5	8.3929	73	−8	−164	2.96	1.87	1.11	0.45
0.6	8.4035	69	−5	−122	3.94	2.58	1.32	0.4

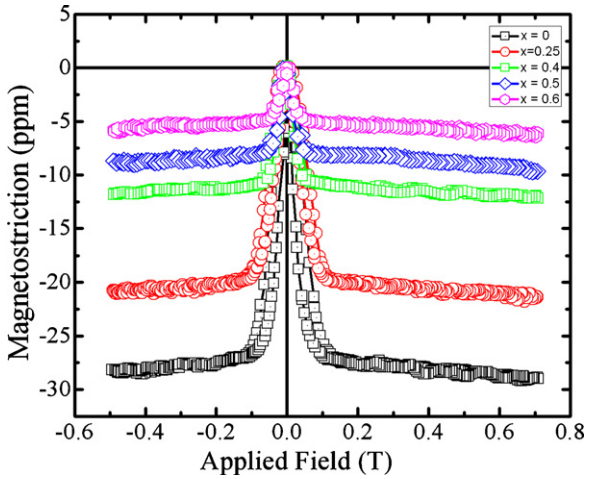

Fig. 3. Linear magnetostriction of $Ni_{1-x}Zn_xFe_2O_4$ measured at room temperature.

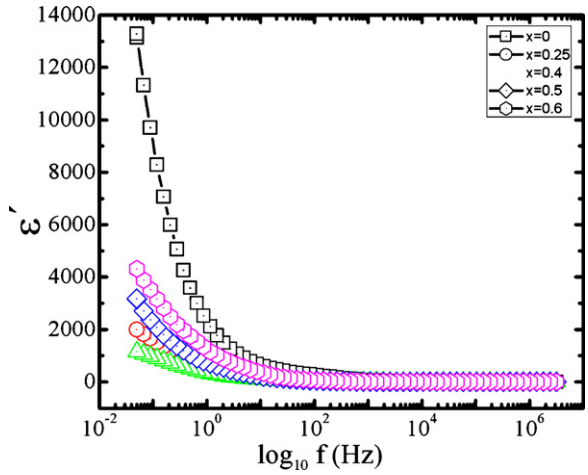

Fig. 4. Variation of dielectric permittivity with frequency for $Ni_{1-x}Zn_xFe_2O_4$ measured at room temperature.

decrease with the further increase in the zinc contents (i.e., $x > 0.4$). This behavior is understood in terms of the exchange interactions such as A–B, A–A and B–B, which depend upon the distribution of magnetic and non-magnetic ions in the spinelic network at A- and B-sites [4,21]. In the spinelic network of the Ni ferrite where the Fe^{3+} ions are equally distributed in tetrahedral (A) and octahedral [B] sites, while the Ni^{2+} ions preferred to be at octahedral [B] sites. Since the Fe^{3+} ions in the A- and B-sites have equal and opposite magnetic moments, they compensate each other and the total magnetic moment is exclusively determined by the Ni^{2+} ions. When non-magnetic Zn^{2+} ions are substituted in place of Ni^{2+} ions, due to their strong preference Zn^{2+} ions are disposed only in the A-sites, which result in the dislocation of Fe^{3+} ions from A- to B-sites. At this stage, the compensation mechanism of the magnetic moments of Fe^{3+} ions at A- and B-sites vanishes (saturated or minimum) due to transfer of some Fe^{3+} ions with large magnetic moments to B-sites, which results in an increase in the magnetization. The magnetization increases with the Zn substitution up to $x = 0.4$ and after reaching the $x = 0.4$ concentration, there takes place a weakening of the A–B exchange interaction, and the parallel orientation of the magnetic moments in the B-sites is altered that compensate each other only partially which leads to a progressive decrease of the saturation magnetization [22].

Longitudinal magnetostriction 'λ' of $Ni_{1-x}Zn_xFe_2O_4$ samples measured at room temperature is shown in Fig. 3. It has been observed that the maximum value of magnetostriction decreases with increasing zinc contents. This behavior of magnetostriction is due to the fact that Ni^{2+} ions has a large orbital moment as compare to Zn^{2+} which has no magnetic moment, so when we substitute Ni^{2+} ions by Zn^{2+} it causes not only a reduction of anisotropy field but also the magnetostriction value [15]. The strain derivative or the slope of the magnetostriction curve $d\lambda/dH$ is also found to be decrease with increasing Zn content, except for $x = 0.4$ where it is found to be larger than that for $x = 0.25$ as shown in Table 1. The slope of magnetostriction $d\lambda/dH$ is related to the stress sensitivity of the magnetization and is important for a high sensitivity of magnetic induction to stress, which makes this material attractive for the use in advanced magnetomechanical stress torque sensors [23].

Fig. 4 shows the frequency dependence of the real part of dielectric permittivity (ε') for all the samples measured at room temperature. It has been seen that for all the samples the dielectric constant decreases with increasing frequency. The dispersion in dielectric constant is rapid at lower frequencies (100 Hz) which is due to interfacial polarization. At higher frequencies due to rotational displacements of the dipoles which results in the orientational polarization, dispersion in dielectric constant becomes small approaches a nearly frequency independent response. With the addition of zinc a visible change in the dispersion frequency can be seen from Fig. 4. The dispersion frequency for $x = 0$ sample is about 10^6 Hz which changed to 10^4 Hz for all Zn doped samples. The observed behavior of the dielectric dispersion can be explained on the basis of Koops theory [24] and Maxwell–Wagner interfacial type of polarization [25]. In this model, a ferrite material is assumed to consist of well-conducting grains separated by less conducting grain boundaries. The electrons reach the grain boundary through hopping and if the resistance of the grain boundary is high enough, electrons pile up at the grain boundaries and produce polarization. However, as the frequency of the applied field is increased, the electrons reverse their direction of motion more often. This decreases the probability of electrons reaching the grain boundary and as a result the polarization decreases. Therefore, the dielectric constant decreases with increasing frequency of the applied field.

In order to understand the conduction mechanism, the frequency dependence of ac conductivity is shown in Fig. 5, in which conductivity shows an increasing trend with frequency for all samples. Since increase in frequency enhances the hopping frequency of the charge carriers, thereby increasing the conductivity. According to Maxwell and Wagner's two-layer model, at lower frequencies the conductivity is due to the resistive grain boundaries while at

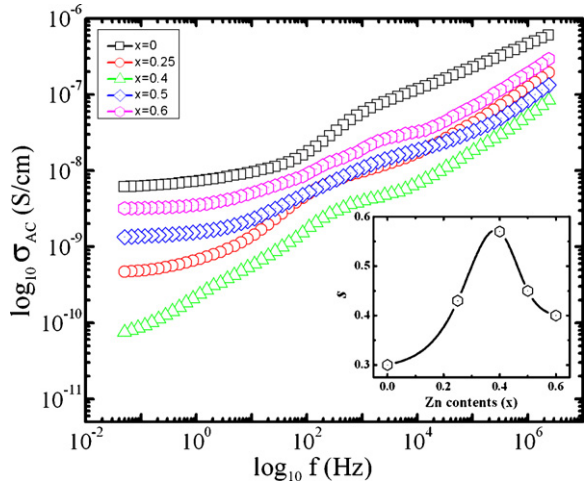

Fig. 5. Variation of AC conductivity with frequency for $Ni_{1-x}Zn_xFe_2O_4$ measured at room temperature. Inset shows variation of exponent s with zinc contents.

higher frequencies conductive grains are more active [25]. It has been observed from Fig. 5 that at low frequency the ac conductivity is found to be weakly frequency dependent for $x = 0$ sample. With increasing zinc contents, there is a visible change in the conductivity behavior from weakly frequency dependence to a strong one. It can be seen that for $x = 0.4$ sample the conductivity becomes a strong function of frequency and the flat curve is unobservable in the low frequency region, whereas above $x = 0.4$ the frequency dependent curve tends to flatten again with increasing zinc contents. The above mentioned observation in conductivity spectra can be explained on the basis of conduction through the grain boundaries. The frequency dependent conductivity curve at low frequency for $x = 0.4$ sample is attributed to the decrease in the hopping frequency due to reduction in the mobility of the charge carriers resulting in an increase in the grain boundary resistance. This decreases the probability of charged carriers crossing over the grain boundary. As a result, the conductivity decreases with increasing zinc content up to $x = 0.4$, where it gets saturated. With the further addition of Zn contents the grain boundary starts to become conducting, which enhances the conduction of charge carriers through the grain boundary thereby increasing the conductivity.

Since AC measurements are an important tool to study the dynamic properties of the semi conducting and dielectric materials. A change in the dispersion frequency has been discussed in the previous paragraph and now in order to find any possible correlation between conductivity and dielectric studies, we employ the power law relation $\sigma = A\omega^s$, where ω is the angular frequency, A is a constant and the exponent s is frequency-dependent parameter and has values less than unity [26]. Using log–log plot of conductivity versus frequency curve shown in Fig. 5, the exponent value s has been calculated at two frequency regions i.e., region-I and region-II, due to different slopes in the conductivity behavior. In the low frequency region-I ($<10^2$ Hz), the exponent s shows a small variation (0.04–0.08) in the frequency dependence due to nonequilibrium occupancy of the trap charges [27]. Only for $x = 0.4$, the frequency dependence of the conductivity can be understood by considering that trapped carriers become part of conduction at low frequencies and the value of slope s is about 0.36. At high frequency region-II ($>10^4$ Hz), where occupancy of the traps centers is reduced and then these trapped carriers will be available for conduction; the values of the exponent s varies in the range of 0.29–0.57. It is therefore viable to compare the trend of slope in a region where these trapped carriers are available for conduction. Inset of Fig. 5 shows the variation of s with zinc contents in the frequency range of 10^4–10^6 Hz. According to Pollak and Geballe developed theory, when charge carriers hop between localized states which are randomly distributed, the ac conductivity is directly proportional to ω^s where $0 < s < 1$ [28]. Since, we are measuring value of slope in the same frequency region for all samples, we observe that for $x = 0.4$ its value shows maxima which is close to universal dielectric response reported in different materials [29]. It has been reported that at room temperature the frequency exponent s either increases or decreases with increasing substitution in ferrites [7,30,31] but we observe a significant variation in the frequency dependence of s as Zn ion substitution increases which might be due to different type of conduction mechanism in the different compositions. To address the conduction mechanism issue (which is beyond the scope of present study) and the nature of localized and delocalized charge carrier further temperature dependent studies will be carried out later on.

The compositional variation of the dielectric permittivity and ac conductivity for $Ni_{1-x}Zn_xFe_2O_4$ at room temperature at 100 Hz, 1 kHz and 10 kHz are shown in Fig. 6. It has been observed that the dielectric permittivity ε' and conductivity σ_{AC} decreases with increasing Zn content up to $x = 0.4$, after which they start to increase

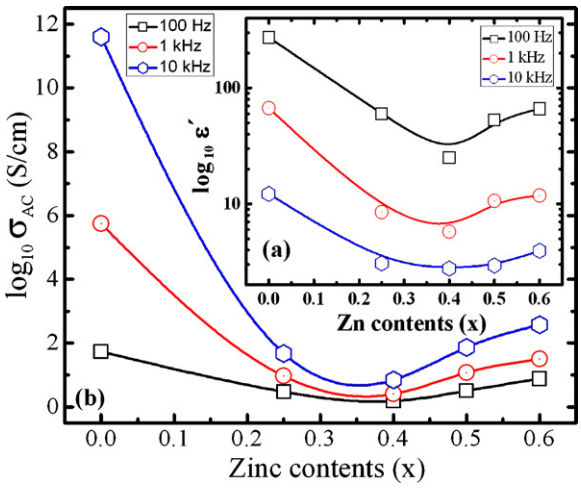

Fig. 6. Compositional variation of (a) dielectric permittivity and (b) ac conductivity at different frequencies for $Ni_{1-x}Zn_xFe_2O_4$.

with further increasing Zn ion substitution. The electric conduction in Ni–Zn ferrites can be explained by the Verwey and de Boer mechanism in which electron exchange between ions of the same element present in more than one valence state takes place [32]. In Ni–Zn ferrite, zinc volatilization at high temperature results in the formation of Fe^{2+} ions and in the same time Ni^{2+} can be oxidized to Ni^{3+} during the sintering process [33,34]. Since Fe^{2+} and Ni^{3+} ions have strong preference to occupy octahedral (B) sites, therefore it is expected that the conduction mechanism occurs as a result of electron exchange between Fe^{2+} and Fe^{3+} ions and hole transfer between Ni^{3+} and Ni^{2+} ions at the octahedral sites [35]. From Fig. 6, it can be seen that the ε' and σ_{AC} becomes largest for the sample with $x = 0$, which means maximum number of Ni^{2+} and Ni^{3+} ions are available for hopping. Hence the main contribution of conductivity may be due to the hole hopping [36]. In Ni–Zn ferrite, the hole conduction depends on the concentration of Zn ions on the A-site to the Ni ion concentration on the B-sites. With increasing Zn^{2+} contents, the number of Ni^{2+} and Ni^{3+} ions on the B-sites decreases. As a result there is a significant decrease in the ε' and σ_{AC} values and we observed a minimum value at $x = 0.4$ which may be attributed to the electron–hole compensation in the B-sites. Further increase of Zn contents diminishes the hole hopping by decreasing the number of ions on the B-site. Thus electron hopping became predominant and it increases the ε' and σ_{AC} values. Therefore the conduction mechanism in samples with low Zn content is predominantly due to hole transfer from Ni^{3+} to Ni^{2+} ions whereas for higher values of Zn the conduction mechanism is due to the hopping of electrons from Fe^{2+} to Fe^{3+} ions at B-sites [6,37].

Fig. 7 shows the variation of the dielectric loss tangent with frequency at room temperature for Ni–Zn ferrite samples. It has been observed that for all samples the loss tangent decreases initially with increasing frequency followed by the appearance of small peaks. These peaks are appearing due to resonance behavior, when the jumping frequency of electrons becomes approximately equal to the frequency of the externally applied alternating electric field. It has been seen that the peak shifts towards lower frequency with increasing zinc content up to $x = 0.4$. However, with a further increase in Zn content (i.e., $x > 0.4$) the peak shifts towards higher frequency. The peak height also decreases with increasing zinc contents. The shift of these relaxation peaks with zinc contents is often attributed to the rate of hopping of charge carriers [38]. Since the number of holes decreases with increasing Zn contents up to $x = 0.4$, which results in a decrease of the mobility of charge carriers therefore the peak shifts towards lower frequency. Whereas for $x > 0.4$,

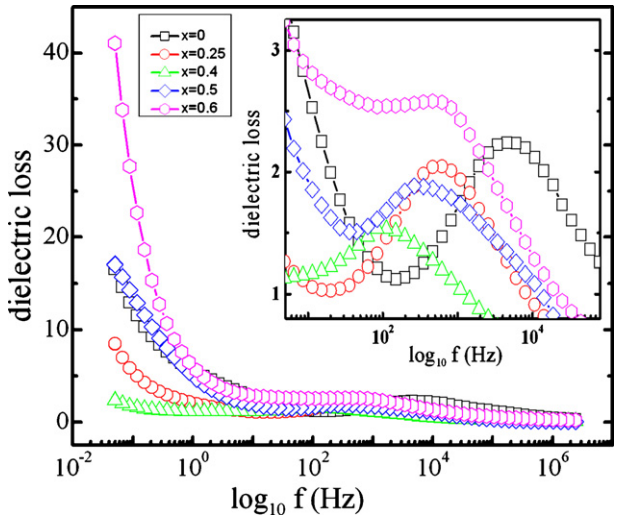

Fig. 7. Variation of dielectric loss tangent with frequency for $Ni_{1-x}Zn_xFe_2O_4$ measured at room temperature.

formation of Fe^{2+} ions increases the hopping frequency of electrons therefore the peaks shifts towards higher frequency.

4. Conclusions

Zinc doped nickel ferrites have been synthesized through a sol–gel method. X-ray diffraction of the prepared samples shows single phase cubic spinel structure. The saturation magnetization increases with increasing Zn contents up to $x = 0.4$, due to an increase in Fe^{3+} ions concentration at the B-sites of the spinelic network. However, with a further increase in the Zn content ($x > 0.4$) magnetization begins to decrease due to the weakening of AB-exchange interaction. The value of magnetostriction decreases due to the substitution of non-magnetic zinc in the nickel ferrite. As the zinc content is increased the dielectric permittivity (ε'), dielectric loss tangent ($\tan\delta$) and AC conductivity (σ_{AC}) decreases, whereas with the further addition of zinc it begins to increase. This variation in the dielectric parameters has been explained on the basis of electron–hole hopping mechanism. From a comparison of the magnetic, magnetostrictive and dielectric properties of the zinc doped nickel ferrite, it has been found that $x = 0.4$ is an optimum composition showing a comparatively high magnetization, low dielectric constant and conductivity, high slope of magnetostriction, which seems to be the suitable constituent phase for magnetoelectric (ME) composites. In future the maximum magnetoelectric output can be obtained by mixing the $x = 0.4$ composition of Ni–Zn ferrite with the suitable ferroelectric phase i.e., PZT which has high piezoelectric coefficient.

Acknowledgment

M. Atif would like to thank Higher Education Commission (HEC) of Pakistan for providing financial support under Overseas Scholarship Scheme (Phase-II) for his PhD studies.

References

[1] J.L. Dorman, D. Fiorani (Eds.), Magnetic Properties of Fine Particles, Amesterdam, North-Holland, 1992.
[2] E.S. Murdock, R.F. Simmons, R. Davidson, IEEE Trans. Magn. 28 (1992) 3078.
[3] V. Uskokovic, M. Drofenik, I. Ban, J. Magn. Magn. Mater. 284 (2004) 294.
[4] J. Smit, H.P.J. Wijn, Ferrites—Physical Properties of Ferrimagnetic Oxides in Relation to Their Technical Applications, N.V. Philip's Gloeilampenfabrieken, Eindhoven/Holland, 1959 (Chap. VIII), pp. 136–176.
[5] M. Ajmal, A. Maqsood, Mater. Lett. 62 (2008) 2077.
[6] A.M. El-sayed, Mater. Chem. Phys. 82 (2003) 583.
[7] A.M. Abdeen, J. Magn. Magn. Mater. 192 (1999) 121.
[8] G. Ranga Mohan, D. Ravinder, A.V. Ramana Reddy, B.S. Boyanov, Mater. Lett. 40 (1999) 39.
[9] A. Verma, T.C. Goel, R.G. Mendiratta, M.I. Alam, Mater. Sci. Eng. B 60 (1999) 156.
[10] H.M. Zaki, J. Phys. B: Condens. Matter 363 (2005) 232.
[11] T. Jahanbin, M. Hashim, K.A. Mantori, J. Magn. Magn. Mater. 322 (2010) 2684.
[12] M.M. Rashad, E.M. Elsayed, M.M. Moharam, R.M. Abou-Shahba, A.E. Saba, J. Alloys Compd. 486 (2009) 759.
[13] A.S. Fawzi, A.D. Sheikh, V.L. Mathe, J. Alloys Compd. 502 (2010) 231.
[14] A.K.M. Akther Hossain, S.T. Mahmud, M. Seki, T. Kawai, H. Tabata, J. Magn. Magn. Mater. 312 (2007) 210.
[15] S.R. Murthy, S.T. Rao, Phys. Status Solidi (A) 90 (1985) 631.
[16] C.W. Nan, M.I. Bichurin, D. Shuxiang, D. Viehland, G. Srinivasan, J. Appl. Phys. 103 (2008) 031101.
[17] R.C. Kambale, P.A. Shaikh, C.H. Bhosale, K.Y. Rajpure, Y.D. Kolekar, Smart Mater. Struct. 18 (2009) 115028.
[18] R. Grössinger, G.V. Duong, R. Sato-Turtelli, J. Magn. Magn. Mater. 320 (2008) 1972.
[19] S. Gautam, A. Thakur, S.K. Tripathi, N. Goyal, J. Non-Cryst. Solids 353 (2007) 1315.
[20] C. Rath, S. Anand, R.P. Das, K.K. Sahu, S.D. Kulkarni, S.K. Date, N.C. Mishra, J. Appl. Phys. 91 (2002) 2211.
[21] R.G. Gupta, R.G. Mendiratta, J. Appl. Phys. 48 (1977) 2998.
[22] C. Caizer, M. Stefanescu, C. Muntean, I. Hrianca, J. Optoelectron. Adv. Mater. 3 (2001) 919.
[23] R. Grössinger, N. Mehmood, G. Senbaslar, A. Muhammad, R. Sato Turtelli, W. Linert, F. Kubel, in: D. Niarchos (Ed.), Proceedings of REPM 2008, 2008, p. 214 (ISBN:978-960-86733r-r6-6).
[24] C.J. Koops, Phys. Rev. 83 (1951) 1520.
[25] K.W. Wanger, Ann. Phys. 40 (1913) 817.
[26] S.R. Elliott, Adv. Phys. 36 (1987) 135.
[27] M. Nadeem, A. Mushtaq, J. Appl. Phys. 106 (2009) 073713.
[28] M. Pollak, T.H. Geballe, Phys. Rev. 122 (1961) 1742.
[29] A.S. Nowick, A.V. Vaysleyb, I. Kuskovsky, Phys. Rev. B 58 (1998) 8398.
[30] M.A. El Hiti, J. Phys. D: Appl. Phys. 29 (1996) 501.
[31] E.V. Gopalan, K.A. Malini, S. Sagar, D.S. Kumar, Y. Yoshida, I.A. Al-Omari, M.R. Anantharaman, J. Phys. D: Appl. Phys. 42 (2009) 165005.
[32] E.J.W. Verwey, J.H. De Boer, Recl. Trav. Chim. Pays-Bas 55 (1936) 531.
[33] L.G. Van Uitert, J. Chem. Phys. 24 (1956) 306.
[34] C. Prakash, J.S. Baijial, J. Less-Common Met. 106 (1985) 257.
[35] P.V. Reddy, T.S. Rao, S.M.D. Rao, J. Less-Common Met. 79 (1981) 191.
[36] S. Sindhu, M.R. Anantharaman, B.P. Thampi, K.A. Malini, P. Kurian, Bull. Mater. Sci. 25 (7) (2002) 599.
[37] R. Satyanarayana, S.R. Murthy, T.S. Rao, J. Less-Common Met. 90 (1983) 243.
[38] N. Rezlescu, E. Rezlescu, Phys. Status Solidi (A) 23 (1974) 575.